On developing a new ionospheric plasma index for the Brazilian equatorial F region irregularities

Laysa Cristina Araujo Resende[1], Clezio Marcos Denardini[1], Giorgio Arlan Silva Picanço[1], Juliano Moro[2], Diego Barros[1], Cosme Alexandre Oliveira Barros Figueiredo[1], Régia Pereira Silva[1].

[1]National Institute for Space Research (INPE) S. J. Campos, SP, Brazil
[2] National Space Science Center, Chinese Academy of Sciences, CAS, Beijing, China & Southern Regional Space Research Center – CRS/INPE, Santa Maria, RS, Brazil

Correspondence to: Laysa C. A. Resende (laysa.resende@inpe.br; laysa.resende@gmail.com)

Abstract. F region vertical drifts (V_z) are the result of the interaction between the ionospheric plasma with the zonal electric field and the Earth's magnetic field. Abrupt variations in V_z are strongly associated with the occurrence of plasma irregularities (spread-F) during the nighttime periods. These irregularities are manifestations of the space weather in the ionosphere environment without necessarily require a solar burst. In this context, the Brazilian Space Weather Study and Monitoring Program (Embrace) of the National Institute for Space Research (INPE) has been developing different indexes to analyze these ionospheric irregularities in the Brazilian sector. Therefore, the main purpose of this work is to produce a new ionospheric scale based on the analysis of the ionospheric plasma drift velocity, named AV. It is based in the maximum value of V_z (V_{zp}), which in turn is calculated through its relationship with the virtual height parameter, *h'*F, measured by the Digisonde Portable Sounder (DPS-4D) installed in São Luís (2°S, 44° O, dip: -2,3°). This index quantifies the time relation between the V_z peak and the irregularity observed in the ionogramas. Thus, in this study, we analyzed 8 years of data, between 2009 and 2015, divided by season in order to construct a standardized scale. The results show there is a delay of at least 15 minutes between V_{zp} observation and the irregularity occurrence. Finally, we believe that this proposed index allow evaluating the impacts of ionospheric phenomena in the Space Weather environment recently.

1

1 Introduction

Ionospheric irregularities or spread-F occur in the F region, which are characterized by regions of signal scattering in ionossondes. In general, the spread-F may be associated to plasma bubbles characterized by regions where the plasma density is reduced. Also, these irregularities usually develop after sunset (Abdu et al., 1983; Abdu, 2001). The plasma bubbles are generated through the nonlinear evolution of the Rayleigh-Taylor Instability in equatorial regions (Bittencourt and Abdu, 1981; Abdu et al., 2006; Huang et al., 2002; Abdu et al. 2009).

The most useful parameter to analyze these irregularities is the vertical drift velocity (V_z), which is response of the zonal electric field in the F region, and it is controlled by the interaction between the E- and F-layers, being positive (upward) during the day. In the nighttime period, the vertical plasma drifts become negative due to the inversion of neutral wind (Abdu et al., 2006). Soon before the inversion, an increase in plasma drift occurs lifting the equatorial F layer and controlling the generation of plasma bubbles (Fejer et al., 1991, 2008, Huang et al., 2002). This phenomenon is named pre-reversal enhancement (PRE) of the vertical plasma drift and gives rise to a maximum in the vertical velocity drift (V_{zp}) around 18:00-19:00 LT (Heelis et al., 1974; Farley et al., 1986).

It is well established that the PRE presents a great variability in relation to seasonality, solar cycle and magnetic activity (Fejer, 1991, Abdu et al., 1995, Fejer et al., 2008). In the Brazilian sector, the ionospheric irregularities occur frequently in summer due to the relatively small angle between the solar terminator and the magnetic meridian (Batista et al., 1986). Therefore, there is an almost instantaneous decoupling between the E and F regions. Thus, the polarization electric fields of the F region associated with the PRE peak have higher amplitudes and, the vertical drift of the plasma reaches higher velocities.

Regarding the solar flux, some works have pointed out a direct correlation between V_z and F10.7 radio index (Fejer et al., 1979, Fejer et al.,1991, Batista et al.,1996). In fact, the number of free electrons in the ionosphere will increase with the solar flux intensification causing intense electric fields. Consequently, larger amplitudes of the V_z parameter are observed.

Although several studies report the plasma irregularities occurrences in the F region with plasma vertical drift increases, there is still no climatological study that related the cause and effect of the solar-terrestrial applied to the ionosphere to construct an ionospheric index. Additionally, there are no indexes

2

related to the irregularities in ionospheric plasma as spread-F (plasma bubbles). Jakowski et al. (2012) suggested a disturbance ionosphere index (DIX), in which it describes the perturbation degree of the ionosphere using the Global Navigation Satellite Systems (GNSS) data. Recently, Nishioka et al. (2017) related the plasma irregularity occurrence using a index based on the Total Electron Content (TEC) measurements. However, we did not found any study about the ionospheric index that related the drift velocity with the irregularity/plasma bubbles occurrences.

Therefore, in this study we present the new developed ionospheric index, AV, based on the V_z parameter. This index quantifies the time relation between the V_z peak, and the irregularity observed in the ionograms. The time relation between these parameters (V_{zp} and irregularity observation) is at least 15 minutes for values of V_{zp} less than 60 m/s. Thus, this study demonstrated that the AV index can be used for Space Weather forecast, and it will help in the evaluation of the phenomena impacts in the ionosphere.

2 Data Set

We have used ionospheric data at the Brazilian sector, São Luís (2° 31' S, 44° 16' W, dip: -2.3°). The data were acquired by a Digisonde Portable Sounder (DPS4), an ionospheric radar that operates in variable high frequency (HF). The data are composed of the signal reflected by the ionospheric layers, in which they are registered in ionograms, graphs of frequency versus virtual height (h'F). Therefore, it is possible to calculate the electron density profile and parameters of the different regions in the ionosphere (Reinisch, 1986; 2009).

The V_z parameter is a representation of the vertical drift velocity of the post-sunset F-region (Bittencourt and Abdu, 1981, Abdu et al., 1983, Abdu et al., 2006). It is important to mention that the heights below 300 km were not considered in this study since the ionosphere plasma is subject to the recombination effects. We have calculated the V_z using its relation with h'F determined as $Vz = \dfrac{\Delta h' F}{\Delta t}$.

The h'F parameter is collected every 15 minutes interval on a continuous basis. We have used h'F values over 18:00-21:00 UT (21:00-24:00 LT) of each night to obtain the V_z parameter for the present analysis.

3

The higher vertical drift velocity in each day, or V_{zp}, is considered to represent the PRE. As the purpose of this analysis is to quantify the time relation between V_{zp} and the ionospheric irregularity occurrences, we firstly analyzed two years representing high (year 2001) and low (descending phase) (year 2015) solar flux. It is important to mention that the criterion was to choose two whole years in different phases of the solar cycle that had a complete and revised amount of data to avoid any error in the results. We used this analysis to construct the AV index scale. In the following step, we performed a climatological study considering the data acquired from the years 2009 to 2014 in order to validate the developed AV scale. Lastly, the dataset was separated in seasons: equinoxes (March, April and May, September, and October), summer (November, December, and January), and winter (June, July, and August), since the irregularities are observed every night between November and January. In other words, since plasma bubbles occur between September and March, we eliminate the two months before and after this analysis. The same criterion was used in the winter season.

3 Results and Discussions

3.1 AV Index Scale

The purpose of this analysis is to quantify the interrelationship between V_{zp} and the ionospheric irregularity occurrences that may be associated with plasma bubbles (spread-F). Based on previous studies about this correlation (Batista et al., 1986, Batista et al., 1996, Abdu et al., 2001), it can be assumed that the lowest and highest variations in the V_{zp} amplitude are, approximately, 20 and 70 m/s, respectively. Therefore, we proposed a scale to quantify the time at which the irregularity occurs after the highest V_{zp} value.

The new ionospheric scale AV is divided into five levels as shown in Table 1. The colors indicate the level of disturbance in increasing order of magnitude. AV_1 and AV_2 (blue/green) imply the typical conditions, when no irregularities in the ionospheric plasma have been observed. From the AV_3 (yellow) and above it is possible to observe the spread in the F region detected by the Digisonde. The AV_4 and AV_5 indexes, represented respectively by orange and red colors, meaning extreme conditions, which the existence of plasma bubbles is more probable. The color selection was used based on the Embrace index development program.

4

Table 1: The ionospheric scale named AV index. Vzp is given in m/s.

AV$_1$	$20 \leq V_{zp} < 30$
AV$_2$	$30 \leq V_{zp} < 40$
AV$_3$	$40 \leq V_{zp} < 50$
AV$_4$	$50 \leq V_{zp} < 60$
AV$_5$	$V_{zp} \geq 60$

It has been known from previous studies that irregularities in F region can be observed when V_{zp} amplitudes are higher than 30 m/s (Abdu et al., 1985; Fejer et al., 1999). In the Brazilian region, Abdu et al. (1983) and Abdu et al. (2009a) found that the V_{zp} should be around 30-50 m/s to observe the irregularity/spread-F. However, other authors found a threshold of 40 m/s in different locations (Basu et al., 1996; Whalen, 2003). Furthermore, the irregularity occurrence probability becomes higher when the V_{zp} is greater than 40 m/s (Huang et al., 2015). In fact, we do not observe in our analysis an expressive irregularity occurrence for V_z less than 40 m/s. Therefore, the threshold was selected as 40 m/s here to validate the proposed AV index.

Since the V_{zp} intensification may indicate the occurrence of plasma irregularities in ionograms, mainly plasma bubbles, we performed a statistical analysis to find the correlation between the instant in which V_{zp} increases with the time that the irregularity is identified. An example is shown in Table 2 for January 11, 2001. It is observed that V_{zp} reaches 53 m/s at 21:45 UT that corresponds to the AV$_3$ index. The irregularity can be observed in the ionogram 45 minutes after the V_{zp} peak (22:30 UT), as shown in Figure 1. The red arrows indicate the spread in the F region.

Table 2 -Example of the relation between the irregularity occurrence and V_{zp} parameter.

Day	Vzp	Index Scale	Time	Spread F Time Occurrence
1101	43	AV$_3$	21:45	22:30

5

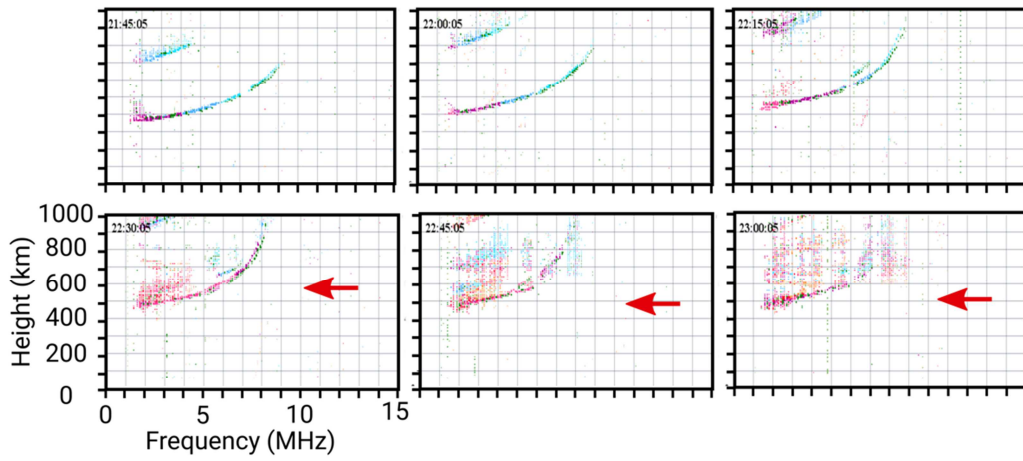**FIGURE 1** – Sequences of ionograms showing the spread-F over São Luís on January 26, 2001 (red arrows).

3.2 AV Index Validation

5   Table 3 presents the statistics of the data used in the analysis for 2001 and 2015, considering the total number of observations, number of days in which the irregularities were observed, and the number of the days that their classification was the AV_3, AV_4 or AV_5.

Table 3 – Statistics of the data used in this study for 2001 and 2015.

Year	Season	Num. of observations	Num. of irregularities	Index	Days per index
2001	Summer	82	66	AV_3	36
				AV_4	25
				AV_5	5
	Equinoxes	167	63	AV_3	41
				AV_4	21
				AV_5	1
	Winter	84	61	AV_3	10
				AV_4	0
				AV_5	0
2015	Summer	84	61	AV_3	29

			AV$_4$	23
			AV$_5$	9
	Equinoxes	153	58	AV$_3$	35
				AV$_4$	21
				AV$_5$	2
	Winter	70	23	AV$_3$	23
				AV$_4$	0
				AV$_5$	0

Figure 2 shows the statistical analysis between the V_{zp} values considering only the indexes AV$_3$, AV$_4$ and AV$_5$ and the time that the irregularity starts to appear in the ionogram. Firstly, the analysis takes into account the data gathered in the summer of 2001 and 2015 over São Luís. The interval between the V_{zp} peak and the observation of the spread-F was discretized into 5 intervals for the sake of the analysis: 0, 15, 30, 45, and ≥60 min. This quantity is called Δt_{vi} hereafter. Notice that this granularity of 15 minutes is a limitation of the Digisonde sampling time and all the occurrences in which Δt_{vi} is higher than 60 minutes were placed on the last interval.
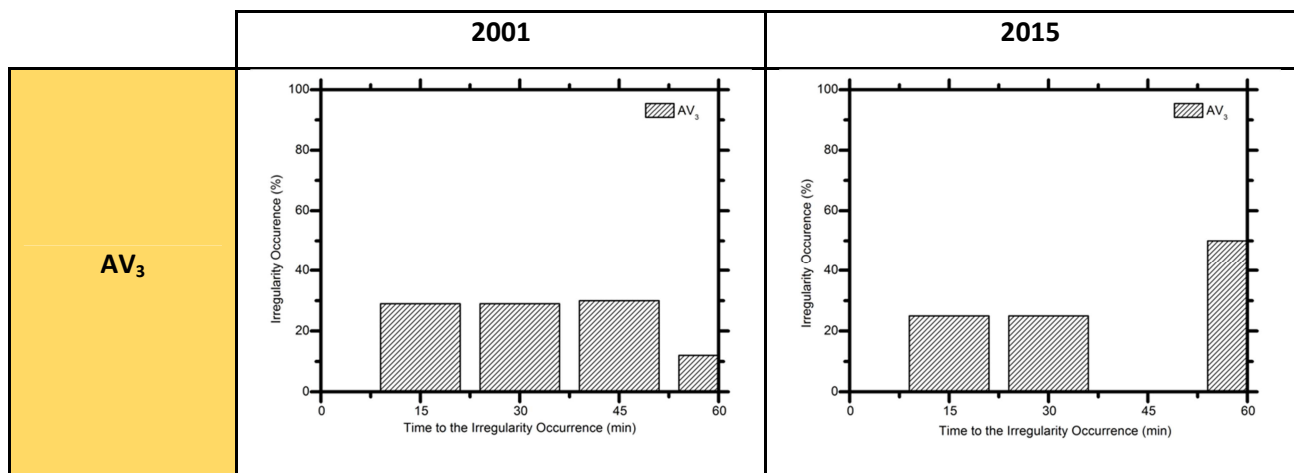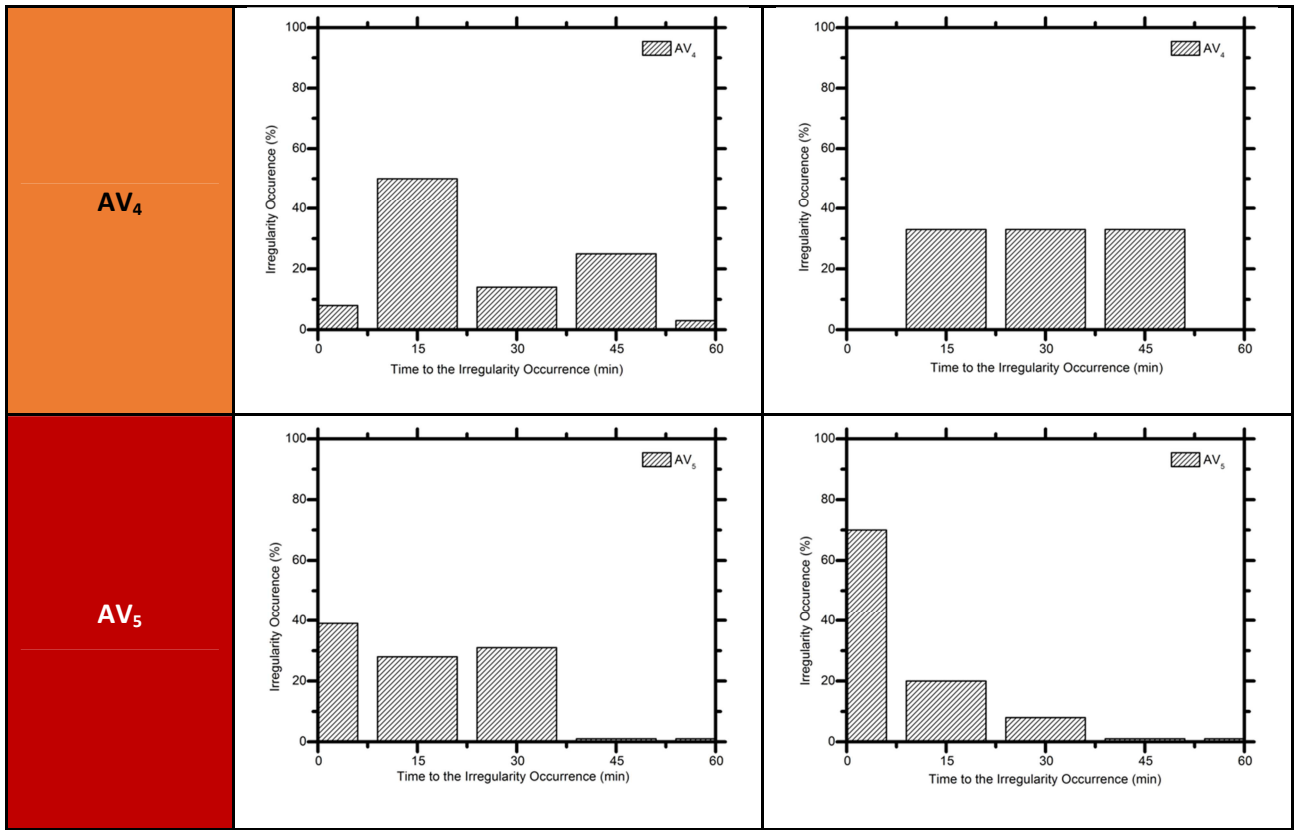
FIGURE 2 – Time relation between the V_{zp} parameter, considering AV_3, AV_4 and AV_5 indexes, and the irregularity observations in ionograms in the summer of 2001 and 2015 over São Luís.

Comparing the results for the AV_3 index, it is observed that Δt_{vi} is at least 15 minutes in both solar cycles. In 2015, no data with Δt_{vi} equal 45 minutes was observed. There was also a significant change comparing both scenarios with respect to the occurrences with Δt_{vi} equal to or greater than 60 minutes. In 2001, only 16% of the cases fell in this interval whereas in 2015 it was 50%.

Regarding the AV_4 index, 10% of the cases had a Δt_{vi} equal to 0 minute during the maximum solar flux (2001), meaning that the spread-F occurred at the same time of the drift velocity peak. On the other hand, in 2015 no data fell into this interval. However, notice that there is a high probability that Δt_{vi} is equal or higher than 15 minutes.

When the index reached the AV_5 corresponding to extreme cases, we observe a high occurrence of events with Δt_{vi} equals 0 minute. In fact, notice that almost 40% of that data in 2001 and 70% of the data in 2015 comprise this interval.

It can be inferred from our results that the probability density function of Δt_{vi} for AV_3 and AV_4 approaches a uniform distribution with lower bound at 15 minutes, except for 2001 and AV_4. Regarding AV_5 in 2001, the distribution seems uniform with lower bound at 0 minute and upper bound at 30 minutes. For the same index, the distribution appears to be exponential in 2015. Furthermore, it can be concluded that the probability to observe Δt_{vi} less than 15 minutes given that the index is AV_3 or AV_4 is negligible.

It is well established that the spread-F occurrence depends on the season and epoch in the solar cycle (Abdu et al., 1983; Abdu et al., 1995; Abdu, 2001). Abdu et al. (1985) showed that the drift velocities were small during the low sunspot years, which weaken the irregularities development. Huang et al. (2002) observed that the maximum irregularities rates were significantly higher during the maximum phase of the solar cycle. This behavior happens because the thermospheric winds and longitudinal gradients in conjugate E layer conductivity are more effective. Those are the key parameters that control the evening F region dynamo electric field. Therefore, during the high solar activity, there are significant variations in thermospheric winds and in longitudinal conductivity gradients of the evening conjugate E layers, which lead to higher values of V_{zp} and, consequently, a favorable environment for the irregularity formation (Abdu et al., 1983).

In our analysis, we observed a significantly high number of irregularities in 2015. We believe that it is caused due to the descending phase of the solar cycle. However, although the irregularities reached the AV_5 level in 2015, its duration in ionograms was lower than that in 2001. This can be seen in Figure 2, where we show the duration of spread-F in ionograms for AV_3 level in 2001 and 2015. The duration of irregularity was divided into 5 intervals: less than 6 hours (t<6), between 6 and 7, 7 and 8, 8 and 9 (6<t<7; 7<t<8; 8<t<9), and $\geq$ 9 hours. The difference between the years is very clear, which in high solar cycle the duration of irregularities is more than 9 hours in most of the events. On the other hand, in 2015 the spread-F last less than 6 hours almost 70% of cases, revealing a solar flux influence and agreeing with the previous study (Abdu et al., 1985; Huang et al., 2002).
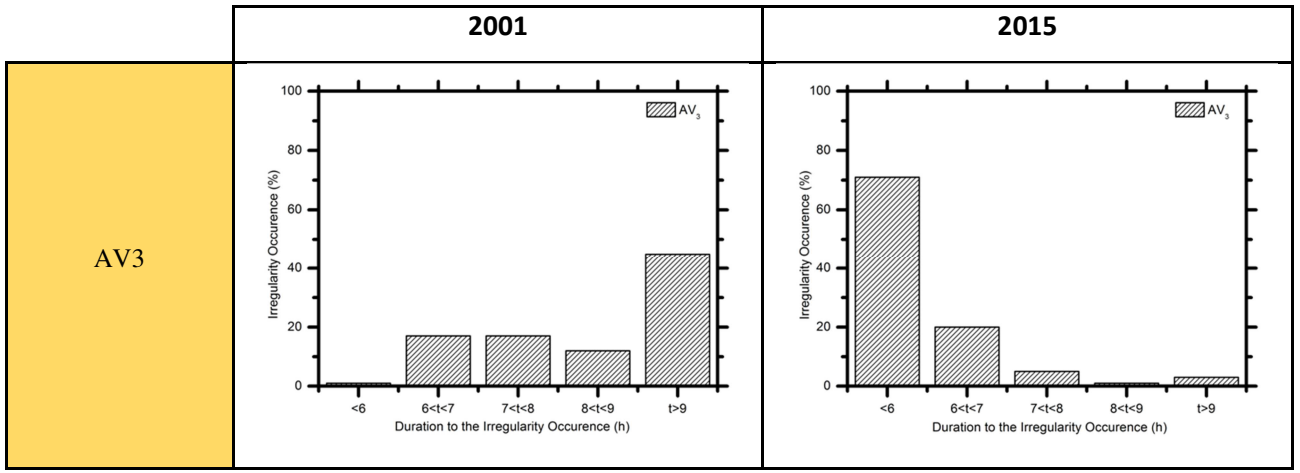
9

FIGURE 3 – Occurrence of spread-F in ionograms for AV_3 index in 2001 and 2015 over São Luís to evidence the differences between the solar flux levels.

In the early hours, the irregularities were controlled by the polarization electric field, but after 6 hours it is the dynamics that controls the bubble (Huang et al., 2011). Barros et al. (2018) show an important role of the zonal wind in the evolution of the plasma bubbles in the TEC data between 2012 and 2016. They did not discuss the differences about the solar cycle phases. However, they showed a good agreement between the zonal drift velocities and the thermospheric winds in the plasma bubbles occurrence. Therefore, we believe that the thermospheric winds in 2015 were lower than 2001 interfering in the growth rate of Rayleigh-Taylor instability (discussed ahead). This fact will be evaluated in greater detail in future work.

As mentioned before, the spread-F is directly related to the plasma bubbles. These plasma bubbles are formed due to the Rayleigh-Taylor gravitational instability process which is operational on the steep upward gradient in the nighttime bottom side of the F region at the magnetic equator (Abdu et al., 2006). This Rayleigh-Taylor mechanism is related to the linear growth rate (γ) given by (Haerendel et al., 1992; Sultan, 1996; Abdu et al., 2001; Abdu et al., 2006)

$$\gamma = \frac{\sum_F P}{\sum_E P + \sum_F P}\left(\frac{E}{B} - U^P + \frac{g}{\nu}\right)\frac{1}{L} - \beta, \qquad (1)$$

10

where the $\sum P$ is the Pedersen conductivity in the field-line integrated for the E and F; U^P is the zonal wind; E and B are the ambient zonal electric field and the magnetic field intensity, g is the gravitational acceleration, ν is the collision frequency, L is the Macllwain parameter, and β is the recombination loss rate. All the terms in this equation were discussed in Abdu (2001). However, we highlight here that the angle formed between the solar terminator and the magnetic meridian is relatively small in summer, and consequently there is an almost instantaneous decoupling between the E and F regions. (Batista et al.,1986). Thus, the polarization electric fields of the F region associated with the V_z peak have higher amplitudes, favoring the instability growth. Thus, the irregularity is most favored to occur in summer than winter (Tsunoda, 1985, Barros et al., 2018).

In order to investigate the seasonal behavior, we analyzed the AV index for equinoxes and winter in 2001 and 2015 over São Luís. The results are presented in Figures 4 and 5 for the equinoxes and winter, respectively.

In relation to equinoxes (Figure 4), the V_{zp} did not reached AV_5 in both years. For AV_4, only few cases were observed in the high solar cycle. Among those, 15% had Δt_{vi} equal 0 minute, 21% had Δt_{vi} equal 15 minutes, 60% had Δt_{vi} equal 30 minutes, and 10% had Δt_{vi} equal 45 minutes. Regarding AV_3, the irregularities were observed between 15 and 45 minutes after V_{zp} peak in both years. No significant values with Δt_{vi} equal 0 minute or greater than 60 minutes were found.
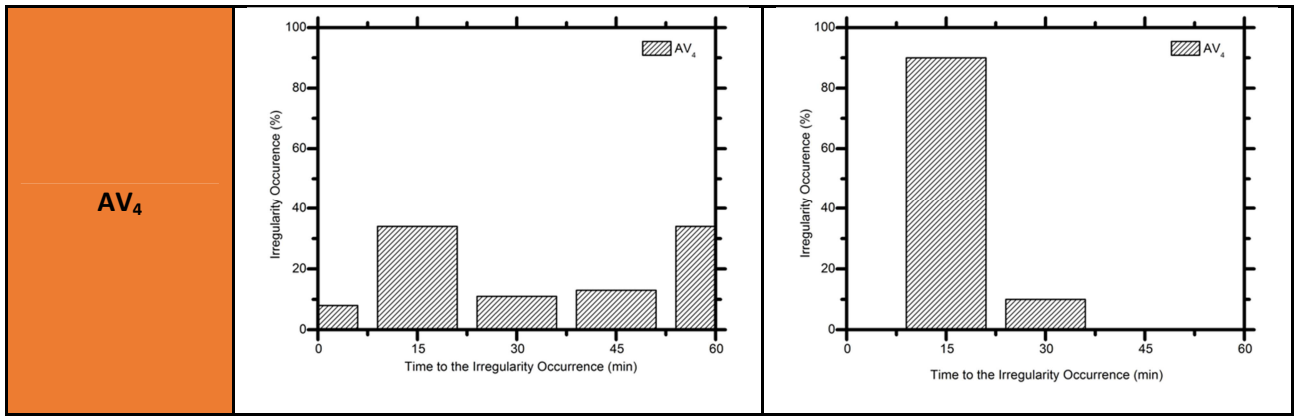

11
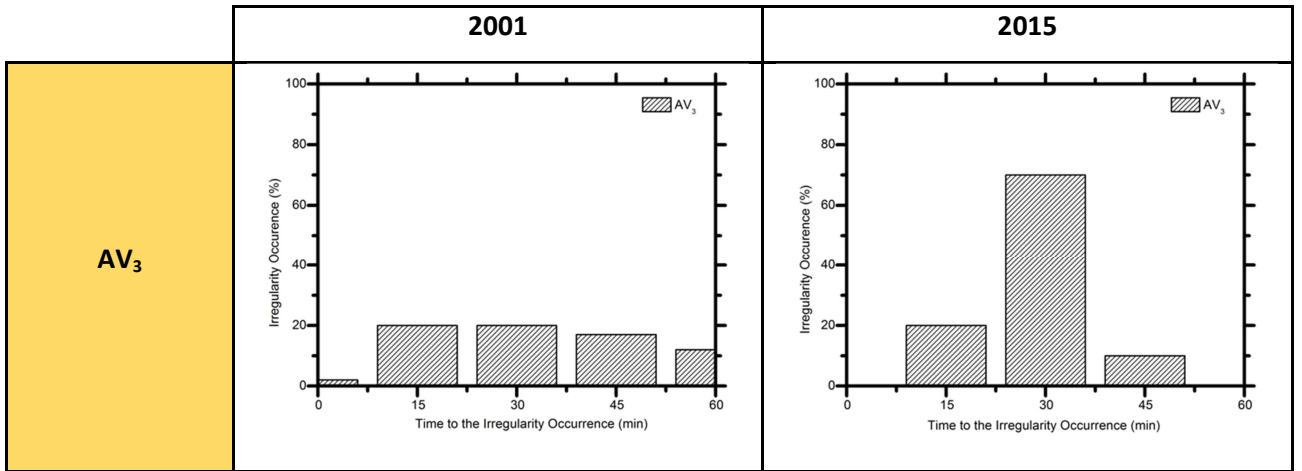
FIGURE 4 – Time relation between the V_{zp} parameter, considering AV3, and AV_4 indexes, and the irregularity observations in ionograms in the equinoxes of 2001 and 2015 over São Luís. The V_{zp} did not reach the AV_5 scale.
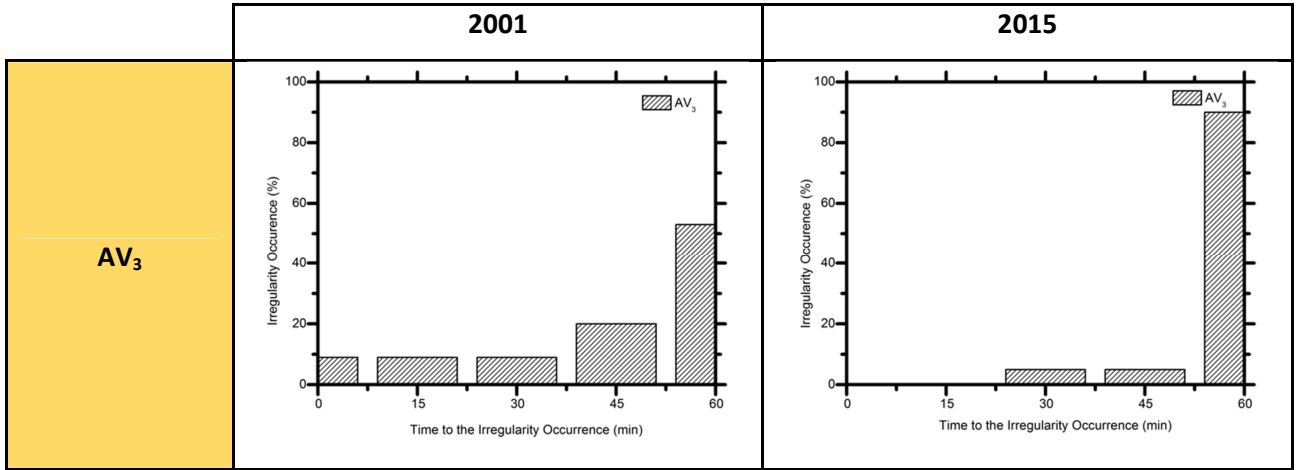

FIGURE 5 – Time relation between the V_{zp} parameter, considering AV_3 index, and the irregularity observations in ionograms in the winter of 2001 and 2015 over São Luís. The V_{zp} did not reach the AV_4 and AV_5 scales.

As seen in Figure 5, the index did not reach AV_4 or AV_5 in winter. In high solar cycle, 10% of the cases had Δt_{vi} equal 0 minute, 10% had Δt_{vi} equal15 minutes, 10% had Δt_{vi} equal 30 minutes, and almost 20% had Δt_{vi} equal 45 minutes. Thus, most of the irregularity observations occurred after one hour from the V_{zp} peak. In the descending phase of the solar cycle in 2015 all irregularities observed in the ionograms had Δt_{vi} equal or greater 60 minutes in AV_3.

Therefore, we observed only few cases of spread-F in both seasons, agreeing with previous studies that irregularities related to plasma bubbles are more frequent in summer (Barros et al., 2018).

12

Thus, we considered the analyze of the summer is enough to validate the proposed AV scale. The climatological results are presented in the following section.
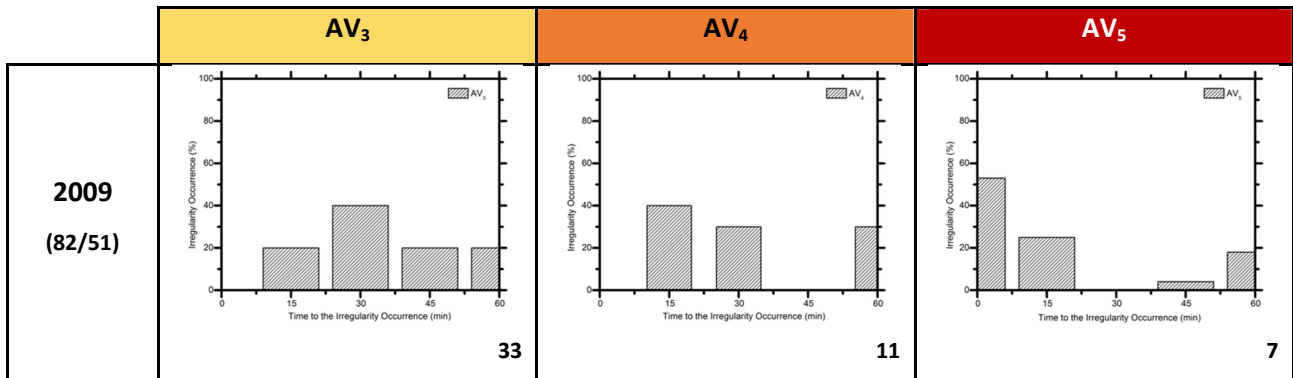
3.3 Climatological study between AV index and spread-F in summer.

Figure 6 shows the relation between V_{zp} intensification, AV index, and the time that the irregularity starts to appear in ionogram. This study considered the data obtained from São Luís station during the summer of 2009 up to 2014. The years 2009 and 2010 refer to the minimum solar cycle 24, 2011 and 2012 were related to the ascending phase of the same solar cycle, and 2013 and 2014 to its maximum. In this figure, we also show the quantity of available observations and the number of days that (below the year). Also, we show the quantity for each scale in the AV index used in this analysis.

It is possible to observe from the results that there is no regular pattern between the highest V_{zp} value and the irregularity observations. However, it is important to mention that the probability to observe Δt_{vi} equal or higher than 15 minutes is still very high in all phases of the solar cycle.

We notice that when the index reached AV_5, there is a high occurrence of events with Δt_{vi} equal 0 minute. This behavior is clearly observed in all years, in which almost 70% of that data felt inside this interval.

According to the AV_3 and AV_4 results, we did not observe significant values with Δt_{vi} equal 0 minute. On the other hand, a high number of observations with Δt_{vi} greater than 60 minutes were found, mainly in 2009, 2010, and 2014. However, most of events were found that Δt_{vi} lies between 30 minutes and greater than 60 minutes, showing the same pattern of the results presented in the previous section.
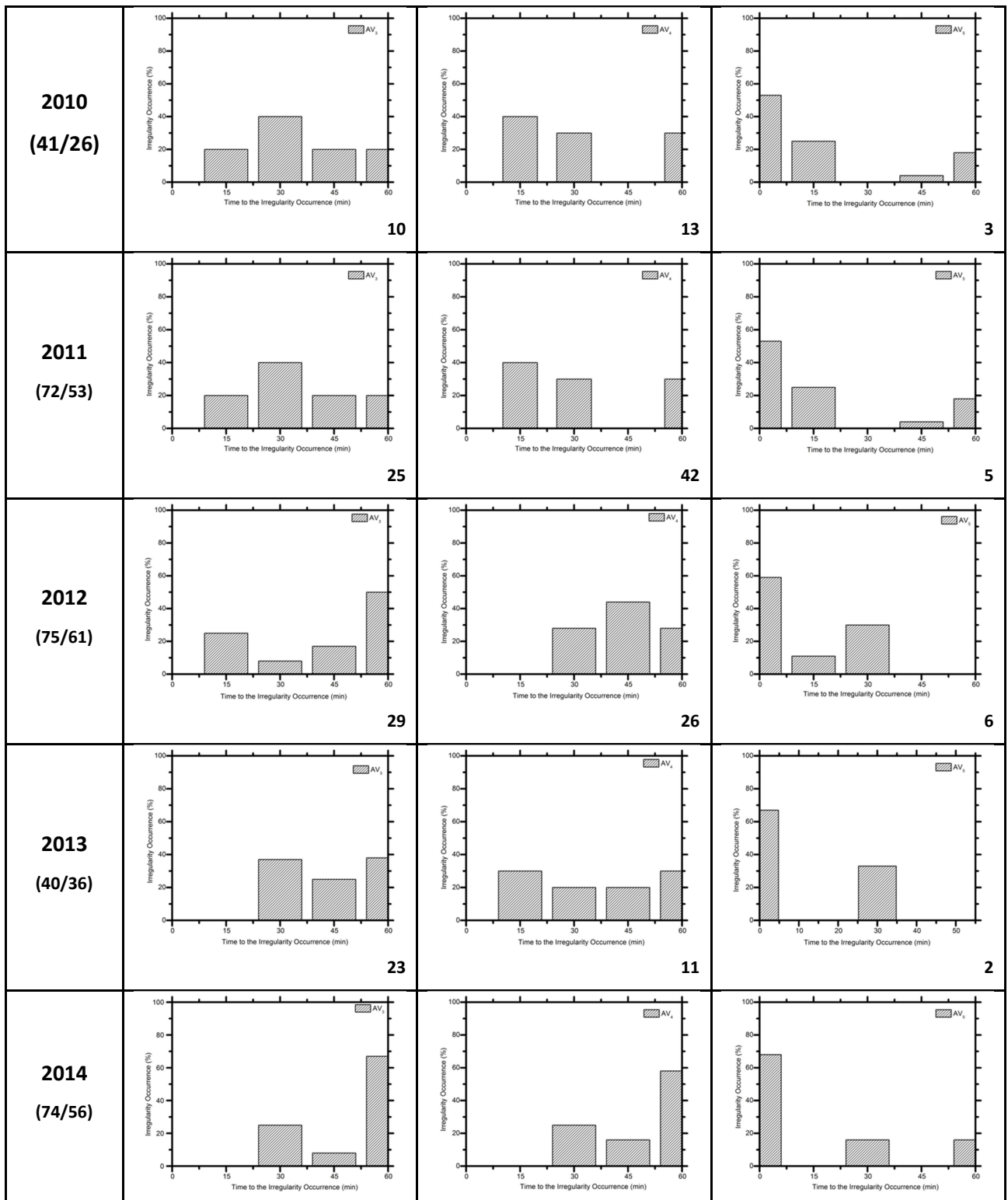

13

2010 **(41/26)**	AV_3 10	AV_4 13	AV_5 3
2011 **(72/53)**	AV_3 25	AV_4 42	AV_5 5
2012 **(75/61)**	AV_3 29	AV_4 26	AV_5 6
2013 **(40/36)**	AV_3 23	AV_4 11	AV_5 2
2014 **(74/56)**	AV_3	AV_4	AV_5

Each cell contains a histogram with y-axis "Irregularity Occurrence (%)" (0–100) and x-axis "Time to the Irregularity Occurrence (min)" (0–60).

	32	20	4

FIGURE 6 – Time relation between the V_{zp} parameter, considering AV_3, AV_4, and AV_5 indexes, and the irregularity observations in ionograms in the summer of 2009 until 2014 over São Luís.

We included an analysis of the average Δt_{vi} considering all years for AV_3 (yellow line), AV_4 (orange line), and AV_5 (red line) in Figure 7. It is possible to observe that the mean Δt_{vi} is greater than 60 minutes, for AV_3 and AV_4. In severe events, *i.e.* AV_5, we had the mean Δt_{vi} equal 0 minute. Thus, we can infer that, under AV_3 and AV_4, the elapsed time between the V_{zp} peak and the irregularity occurrence is greater than 60 minutes with very high probability (around 50%).
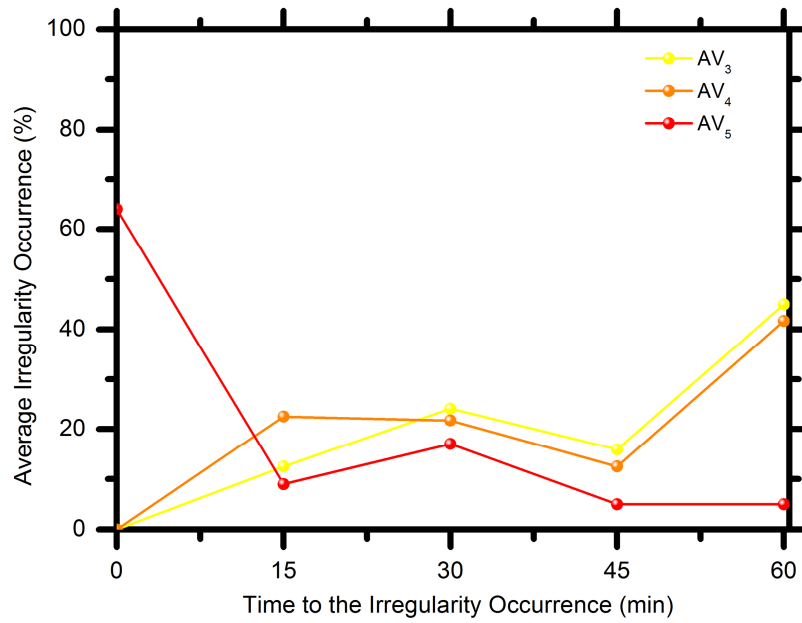

FIGURE 7 - Average time relation between the V_{zp} parameter, considering AV_3 (yellow), AV_4 (orange), and AV_5 (red) indexes, and the irregularity observations in ionograms in summer during 2009 until 2014 over São Luís.

It is well known that the $\frac{E}{B}$ term in Equation 1 arises from the evening vertical drift enhancement (PRE) [Abdu, 2019b]. Therefore, when the height of the F layer is above 300 km, this term ($\frac{E}{B}$) is aproximately equal to V_{zp} [Bittencourt and Abdu, 1981; Batista et al.,1986]. Furthermore, the term $\frac{g}{v}$

15

can suffer a enhancement due to a large V_{zp}, then contributing to an enhancement of the linear growth rate (γ). In other words, the V_{zp} alteration will consequentely an modification in the linear growth rate (γ).

Using data from ground based experiments conducted during the 2005 SpreadFEx campaign in Brazil, Abdu et al. (2009b) shown few case studies where is possibles to see a relationship between V_{zp} and plasma bubble occurrence. The authors observed that the spread-F occurs 30 minutes after the V_{zp} reached values around 40 m/s. They concluded that the relationship between V_{zp} and plasma bubble occurrence is an significative factor to understand the development of these irregularities. Moreover, several authors have reported the necessity to have a wave-like perturbations to trig the Rayleigh-Taylor instability, responsible for the plasma irregularities formation in the F region (Abdu et al., 2009c; Tsunoda, 2006). However, the exact explanation about the time difference between V_{zp} and irregularities occurrence is an open question. Based on previous works cited before, we believed that the wave-like perturbations modified the terms in the Equation 1 may cause this difference. Nevertheless, this subject is out of the scope of this paper. Here, the focus of our discussion is on development of a new ionospheric index.

Finally, to the best knowledge of the authors, there is no ionospheric index in the available literature that related the drift velocity with the irregularity/plasma bubbles occurrences. The ionospheric indexes found are related to the TEC or satellites measurements with the plasma irregularity occurrence (Huang et al., 2015; Nishioka et al., 2017). Additionally, this study confirms that this proposed index can be used to warn the users about the irregularity occurrences, since it was shown that under AV_3 and AV_4 there is at least 15 minutes between V_{zp} peak observation and the irregularity occurrence, with a high probability of the Δt_{vi} to be greater than 60 minutes. Lastly, the AV index is suitable to be incorporated into the products offered by the Embrace program, and it will help in the evaluation of the phenomena impacts in the Space Weather environment.

4 Conclusions

In this study, we develop an ionospheric index, AV, based in the V_z parameter in the F region. The index quantifies the time relation between V_{zp} and the ionospheric irregularity occurrences that may

be associated with plasma bubbles, Δt_{vi}. We analyzed two years representing the different solar flux, 2001 and 2015 to construct the AV index scale. After, we performed a climatological study of 2009 until 2014, in which to validate the AV scale.

In general, the results show that Δt_{vi} is at least 15 minutes in both solar cycles for AV_3 and AV_4 indexes. However, when the index reached the AV_5, in which it is considered extreme events, we observed a high occurrence of events with Δt_{vi} equal 0 minute (60% of the cases).

Additionally, we observed a significantly high number of irregularities in 2015 (61 cases in summer; 58 in equinoxes, and 23 in winter). We attributed this fact due to the descending phase of the solar cycle. However, although the irregularities reached AV_5 in 2015, its duration in ionograms was lower than that in 2001. We believe that the thermospheric winds is the responsible for this behavior, since they interfere in the growth rate of Rayleigh-Taylor instability. This fact will be evaluated in greater detail in future work.

We performed a climatological study during the summer since this season is more significant in spread-F occurrences. Thus, we considered the data obtained from São Luís station of 2009 up to 2014, covering almost the solar cycle. We show an irregular pattern between the highest V_{zp} value and the irregularity observations. However, it is important to mention that the probability to observe Δt_{vi} equal or higher than 15 minutes is still very high in all phases of the solar cycle. In fact, we can infer that, under AV_3 and AV_4, the elapsed time between the V_{zp} peak and the irregularity occurrence is greater than 60 minutes with very high probability.

Finally, we believe that this proposed index can be used to warn the users about the irregularity occurrences, since it was shown that under AV_3 and AV_4 there is at least 15 minutes between V_{zp} peak observation and the irregularity occurrence, with a high probability of the Δt_{vi} to be greater than 60 minutes. And, we did not found any study about the ionospheric index that related the drift velocity with the irregularity/plasma bubbles occurrences as shown in this work. Thus, the AV index is suitable to be incorporated into the products offered by the Embrace program, and it will help in the evaluation of the phenomena impacts in the Space Weather environment.

17

Acknowledgments

References

Abdu, M. A., Medeiros, R. T., Bittencourt, J. A., Batista, I. S. Vertical ionization drift velocities and range spread F in the evening equatorial ionosphere. Journal of Geophysical Research v. 88, p. 399-402, doi.org/10.1029/JA088iA01p00399, 1983.

Abdu, M. A., Sobral, J. H. A., Nelson, O. R., Batista, I. S. Solar cycle related range type spread-F occurrence characteristics over equatorial and low latitude stations in Brazil, Journal of Atmospheric and Terrestrial Physics, v. 47, n. 10, p. 901-905, 10.1016/0021-9169(85)90065-0, 1985.

Abdu, M. A., Batista, I. S., Walker, G. O., Sobral, J. H. A., Trivedi, N. B., De Paula, E. R. Equatorial Ionospheric Electric Fields During Magnetospheric Disturbances: Local Time/Longitude Dependences from Recent EITS Campaigns. Journal of Atmospheric and Terrestrial Physics, v. 57, n. 10, p. 1065-1083, 10.1016/0021-9169(94)00123-6, 1995.

Abdu, M. A. Outstanding problems in the equatorial ionosphere- thermosphere electrodynamics relevant to spread F, Journal of Atmospheric and Terrestrial Physics, 63, p. 869-884, 10.1016/S1364-6826(00)00201-7, 2001.

Abdu, M. A. Equatorial ionosphere-thermosphere system: Electrodynamics and irregularities. Advances in Space Research, v. 35, n.5, p.771-787, 10.1016/j.asr.2005.03.150, 2005.

Abdu, M. A., Batista, P. P., Batista I. S., Brum, C. G. M., Carrasco, A. J., Reinisch, B. W. Planetary wave oscillations in mesospheric winds, equatorial evening prereversal electric field and spread F. Geophysical Research Letters, v. 33, n. 7, p. 1-4, 10.1029/2005GL024837, 2006.

Abdu, M., Kherani, A. E. A., Batista, I. S., Sobral, J. H. A. Equatorial Evening Prereversal Vertical Drift and Spread F Suppression by Disturbance Penetration Electric Fields. Geophysical Research Letters, v. 36, L19103, 5 PP, 10.1029/2009GL039919, 2009a.

Abdu, M. A., Alam Kherani, E., Batista, I. S., de Paula, E. R., Fritts, D. C., Sobral, J. H. A. Gravity wave initiation of equatorial spread F/plasma bubble irregularities based on observational data from the SpreadFEx campaign, Annalles Geophysicae, v. 27, p. 2607-2622, 10.5194/angeo-27-2607-2009, 2009b.

Abdu, M. A., Batista, I. S., Reinisch, B. W., de Souza, J. R., Sobral, J. H. A., Pedersen, T. R., Medeiros, A. F., Schuch, N. J., de Paula, E. R., Groces, K. M. Conjugate Point Equatorial Experiment (COPEX) campaign in Brazil: Electrodynamics highlights on spread F development conditions and day□to□day variability. Journal of Geophysical Research v. 114, A04308, doi:10.1029/2008JA013749, 2009c.

Batista, I. S., Abdu, M. A., Bittencourt, J. A. Equatorial F-region vertical plasma drifts: Seasonal and Longitudinal Asymmetries in the American Sector. Journal of Geophysical Research, v. 91, n. A11, p. 12055-12064, 10.1029/JA091iA11p12055, 1986.

Batista, I. S., De Medeiros, R. T., Abdu, M. A., De Sousa, J. R., Bailey, G. J., De Paula, E. R. Equatorial ionosphere vertical plasma drift model over the Brazilian region. Journal of Geophysical Research, v. 101, n. A5, p. 10887–10892, 10.1029/95JA03833, 1996.

Basu, S., Kudeki, E., Valladares, C. E., Weber E. J., Zengingonul, H. P., Bhattacharyya, S., Sheehan, R., Meriwether, J. W., Biondi, M. A., Kuenzler, H., Espinoza, J. Scintillations, plasma drifts, and neutral winds in the equatorial ionosphere after sunset, Journal of Geophysical Research, v. 101, n. 26, p. 795-809, 10.1029/96JA00760, 1996.

Barros D., Takahashi H., Wrasse C. M. , Figueiredo C. A. O. B. Characteristics of equatorial plasma bubbles observed by TEC map based on ground-based GNSS receivers over South America. Annalles Geophysicae, v. 36, p. 91-100, 10.5194/angeo-36-91-2018, 2018.

Bittencourt, J. A., Abdu, M. A. Theoretical Comparison between Apparent and Real Vertical Ionization Drift Velocities in the Equatorial F-Region. Journal of Geophysical Research, v. 86, n. A4, p. 2451-55, 10.1029/JA086iA04p02451, 1981.

Farley, D. T., Bonelli, E., Fejer, B. G., Larsen, M. F. The prereversal enhancement of the zonal electric field in the equatorial ionosphere, Journal of Geophysical Research, v. 91, n. A12, p. 13723-13728, 10.1029/JA091iA12p13723,1986.

Fejer, B. G., Farley, D.T., Woodman, R. F., Calderon, C. Dependence of equatorial F region vertical drifts on season and solar cycle. Journal of Geophysical Research, v. 84, n.A10, p. 5792-5796, 0.1029/JA084iA10p05792,1979.

Fejer, B. G., Low latitude electrodynamic plasma drifts: A review, Journal of Atmospheric and Terrestrial Physics., 53, n.8, p. 677-693, 10.1016/0021-9169(91)90121-M, 1991.

Fejer, B.G., Scherliess, L., De Paula, E. R. Effects of the vertical plasma drift velocity on the generation and evolution of equatorial spread F. Journal of Geophysical Research, v. 104, n. A9, p. 19,854-19,869, 10.1029/1999JA900271, 1999.

Fejer, B. G., Jensen, J. W., Su, S. Y. Seasonal and longitudinal dependence of equatorial disturbance vertical plasma drifts, 10.1029/2008GL035584, Geophysical Research Letters, v. 35, L20106, 2008.

Haerendel, G., Eccles, J., Cakir, S. Theory of modeling the equatorial evening ionosphere and the origin of the shear in the horizontal plasma flow. Journal of Geophysical Research, v. 97, p. 1209-1223, 10.1029/91JA02226, 1992.

Heelis, R. A., Kendall, P. C., Moffet, R. J., Windle, D. W., Rishbeth, H. Electrical coupling of the E- and F- region and its effects on the F-region drifts and winds, Planetary Space Science, v. 22, n. 5, p. 743-756, 10.1016/0032-0633(74)90144-5, 1974.

Huang, C. Y., Burke, W. J., Machuzak, J. S., Gentile, L. C., Sultan, P. J. Equatorial plasma bubbles observed by DMSP satellites during a full solar cycle: Toward a global climatology, Journal of Geophysical Research, v. 107, n. A12, p.1434, 10.1029/2002JA009452, 2002.

Huang, C. S., Beaujardiere, O., Roddy, P. A., Hunton, D. E., Pfaff, R. F., Valladares, C. E., Ballenthin, J. O. Evolution of equatorial ionospheric plasma bubbles and formation of broad plasma depletions

measured by the C/NOFS satellite during deep solar minimum, Journal of Geophysical Research: Space Physics. v.116, A03309, 10.1029/2010JA015982, 2011.

Huang, C. S., Hairston, M. R. The post-sunset vertical plasma drift and its effects on the generation of equatorial plasma bubbles observed by the C/NOFS satellite, Journal of Geophysical Research: Space Physics, v. 120, p. 2263-2275, 10.1029/2010JA015982, 2015.

Jakowski, N., Borries, C., Wilken, V. Introducing a disturbance ionosphere index, Radio Science, v. 47, RS0L14, 10.1029/2011RS004939, 2012.

Nishioka, M., Tsugawa, T., Jin, H., Ishii, M. A new ionospheric storm scale based on TEC and foF2 statistics, Space Weather, v.15, 10.1002/2016SW001536, 2017.

Maruyama, T. A diagnostic model for equatorial spread F 1. Model description and application to electric field and neutral wind effects. Journal of Geophysical Research, v. 93, p. 14611-14622, 10.1029/JA093iA12p14611, 1988.

Reinisch, B. W. New techniques in ground-based ionospheric sounding and studies. Radio Science, v. 21, n. 3, p. 331-341, 10.1029/RS021i003p00331, 1986.

Reinisch, B. W., Galkin, I. A., Khmyrov, G. M. New Digisonde for research and monitoring applications. Radio Science, p. 44, 10.1029/2008RS004115, 2009.

Sultan, P. J. Linear theory and modeling of the Rayleigh–Taylor instability leading to the occurrence of equatorial spread F. Journal of Geophysical Research v.101, p. 26875-26891, 10.1029/96JA00682, 2006.

Tsunoda, R. T. Control of the seasonal and longitudinal occurrence of equatorial scintillation by longitudinal gradient in integrated Pedersen conductivity. Journal of Geophysical Research v. 90, p. 447-456, 10.1029/JA090iA01p00447, 1985.

Tsunoda, R. T. Day-to-day variability in equatorial spread F: Is there some physics missing? Geophysical Research Letters, v. 33, L16106, 5 PP, 10.1029/2006GL025956, 2006.

Whalen, J. A. Dependence of the equatorial anomaly and of equatorial spread F on the maximum prereversal E × B drift velocity measured at solar maximum, Journal of Geophysical Research, v. 108, n. (A5), p. 1193, 10.1029/2002JA009755, 2003.

21